Avrupa Bilim ve Teknoloji Dergisi
Sayı 20, S. 351-359, Aralık 2020

Araştırma Makalesi

www.ejosat.com ISSN:2148-2683

European Journal of Science and Technology
No. 20, pp. 351-359, December 2020

Research Article

Solvent Effects on the Contrast Agent Iomeprol with Density Functional Theory

Sedat Giray Kandemirli[1], Fatma Genç[2], Fatma Kandemirli[3] and Meryem Evecen [4*]

[1]University of Iowa, Roy Carver College of Medicine, Departmant of Radiology, United States, (ORCID: 0000-0002-3976-4062), gskandemirli@yahoo.com;
[2]Istanbul Yeni Yuzyil University, Departmant of General Chemistry, İstanbul, Turkey, (ORCID: 0000-0002-5304-5347), fatma.genc@yeniyuzyil.edu.tr
[3]Kastamonu University, Departmant of Biomedical Engineering, Kastamonu, Turkey, (ORCID: 0000-0001- 6097-2184), fkandemirli@yahoo.com
[4*]Amsya University, Faculty of Arts and Sciences, Departmant of Physics, Amsya, Turkey, (ORCID: 0000-0001-7926-1323), meryem.evecen@amasya.edu.tr

(First received 5 May 2020 and in final form 13 October 2020)

(**DOI:** 10.31590/ejosat.732239)

ATIF/REFERENCE: Kandemirli, S. G., Genç, F., Kandemirli, F. & Evecen, M. (2020). Solvent Effects on the Contrast Agent Iomeprol with Density Functional Theory. *European Journal of Science and Technology*, (20), 351-359.

Abstract

Contrast compounds, also called contrast agents or contrast media are substances that temporarily change the way X-rays or other imaging tools interact with the body. Iomeprol is a nonionic monomeric iodinated contrast medium. Optimized geometries of Iomeprol, HOMO-LUMO energy, energy gap, global chemical indices, total energy, nonlinear optical and Natural Bond Orbital (NBO) analysis in the gas phase and in solvents (chloroform, acetic acid, ethanol, DMF, DMSO and water) were obtained based on Density Functional Theory with B3LYP/lanl2dz basis set. The results revealed that the solvents have an effect on the optimized and some chemical parameters (hardness, electronegativity, electrophilicity index, nucleofugality,..). It was observed E_{HOMO} values become more negative and E_{LUMO} values become more positive due to the increase dielectrical constant of the solvent. It was observed that Iomeprol had a highest stability, harder and less reactive in the water phase. In the NBO analysis, interaction between donor and acceptor electrons was effected with the dielectric constant of the solvent.

Keywords: Density Functional Theory, Gaussian 09, HOMO-LUMO, Stabilisation Energy, Iomeprol.

Yoğunluk Fonksiyonel Teorisi ile Kontrast Madde Iomeprol Üzerinde Çözücü Etkileri

Öz

Kontrast maddeleri veya kontrast madde olarak da adlandırılan kontrast bileşikleri, X-ışınlarının veya diğer görüntüleme araçlarının vücutla etkileşimini geçici olarak değiştiren maddelerdir. Iomeprol, noniyonik bir monomerik iyotlu kontrast ortamıdır. Iomeprol'ün gaz fazında ve farklı çözeltilerde (kloroform, asetik asit, etanol, DMF, DMSO ve su) optimize olmuş geometrileri, HOMO-LUMO enerjisi, enerji aralığı, global kimyasal indeksler, toplam enerji, doğrusal olmayan optik ve Doğal Bağ Orbital (NBO) analizi Yoğunluk Fonksiyonel Teorisi kullanılarak B3LYP/lanl2dz temel seti ile elde edildi. Optimize edilmiş ve bazı kimyasal parametreler (sertlik, elektronegatiflik, elektrofiliklik indeksi, nükleojenite,..) üzerinde çözücülerin bir etkiye sahip olduğu görülmüştür. Çözücü dielektrik sabitinin artmasıyla E_{HOMO} değerlerinin daha negatif ve E_{LUMO} değerlerinin daha pozitif olduğu gözlenmiştir. Iomeprolün su fazında en yüksek stabiliteye sahip, daha sert ve daha az reaktif olduğu bulunmuştur. Ayrıca NBO analizinde, alıcı ve verici elektronları arasındaki etkileşim, çözücünün dielektrik sabitinden etkilenmiştir.

Anahtar Kelimeler: Yoğunluk Fonksiyonel Teorisi, Gaussian 09, HOMO-LUMO, Stabilizasyon Enerjisi, Iomeprol.

[*] Corresponding Author: meryem.evecen@amasya.edu.tr

1. Introduction

Contrast agents are iodine-containing solutions and the most commonly used in radiology today. Iodinated contrast agents can be used pretty much anywhere in the body and administered as intravenously, intraarterially, intrathecally and intraabdominally [1].

A structure in the human body can be made visible by radiation only if its attenuation of radiation differs from that of its surroundings. The attenuation difference between the different structures is an important effect of the contrast agent, which enhances the attenuation difference between different body structures with different concentrations in the diverse body parts in question. Since the contrast agent is distributed to both the extracellular area and to a lesser extent the intracellular area, it touches all plasma proteins and all cells of the body. Therefore, undesirable adverse reactions may ocur [2]. Although serious or life-threatening reactions can occur, they are usually safe and side effects are usually mild and self-limiting [1].

Contrast agents are classified as ionicmonomers, ionic dimers, nonionic monomers, nonionic dimers and are different in terms of carboxyl and hydroxyl groups and osmolality. In imaging studies, iodinated contrast media are used commonly [3].

Iomeprol is a new nonionic, hydrosoluble, monomeric iodinated, injectable contrast agent with very low molecular toxicity for diagnostic radiologic examinations and Bracco synthesized and developed it. Chemically, Iomeprol is characterized as N1,N1-bis-(2,3-dihydroxypropyl)-5-[(hydroxyacetyl)methylamino]-2,4,6-triiodo-1,3-benzenedicarboxamide [4]. Formulations of iodine do not contain chelants and are characterised by the lowest osmolality, chemotoxicity and viscosity of all the available nonionic, monomeric contrast agent at alike iodine concentrations [5]. Since Iomeprol does not have chelating agent, it causes undesirable hemodynamic and electrophysiological effects less with its lowered ionized calcium in myocardial capillary and interstitial fluid with chelating elements. However, this did not provide advantage over Iomeprol when compared with other nonionic agents in clinical trials [6]. The contrast enhancing potency of Iomeprol is caused by the iodine-trisubstituted benzene ring4. When compared to nonionic contrast agents, it is reported that water solubility is higher with Iomeprol [3]. The 3 high-hydrophilic side-chain groups in structure cause water solubility [4]. Iomeprol is higly soluble in water and forms stable formulation. For this reason, Iomeprol is used for diagnostic procedures because of its many concentrations [7].

Iomeprol has equal diagnostic efficacy and tolerability profile, which is similar to other nonionic contrast agents. Iomeprol is suitable for use in diagnostic imaging like others of its class [3].

2. Material and Method

Gaussian 09 package was used for all calculations [8]. The molecular structure geometries and electronic structure were visualized by GaussView 5.0 program [9]. Optimization for geometry was made by using hybrid 3-parameter exchange function of Becker and nonlocal correlation functional of Lee, Yang, and Parr (B3LYP) [10]. The population analysis has also been performed by the natural bond orbital method at B3LYP/lanl2dz level of theory using natural bond orbital (NBO) program with Gaussian 09.

3. Results and Discussion

The ionization potentials (IP) and electron affinities (EA) of the molecule in the gas phase and in solvents are calculated with the use of Koopman's Hypothesis, including the HOMO and LUMO energy orbitals respectively using the following expressions;

$$IP = -E_{HOMO} \quad (1)$$

$$EA = -E_{LUMO} \quad (2)$$

Figure 1, presents optimised structure, the highest occupied molecular orbital (HOMO), the lowest unoccupied molecular orbital (LUMO) and electron density of Iomeprol in the gas phase computed at the DFT/B3LYP level with the lanl2dz basis set. It can be observed from Figure 1, HOMO are formed from bensene ring and group attached to N atom, bensene ring. LUMO are composed of bensene and iodine groups attached to bensene ring.

HOMO that is an electron donor shows the ability to give electron, the higher the E_{HOMO}, the easier it is for HOMO to give electrons; and LUMO that is an electron acceptor shows the ability to receive electron. If E_{LUMO} is lower, it is the easier to accepts electrons for the LUMO [11].

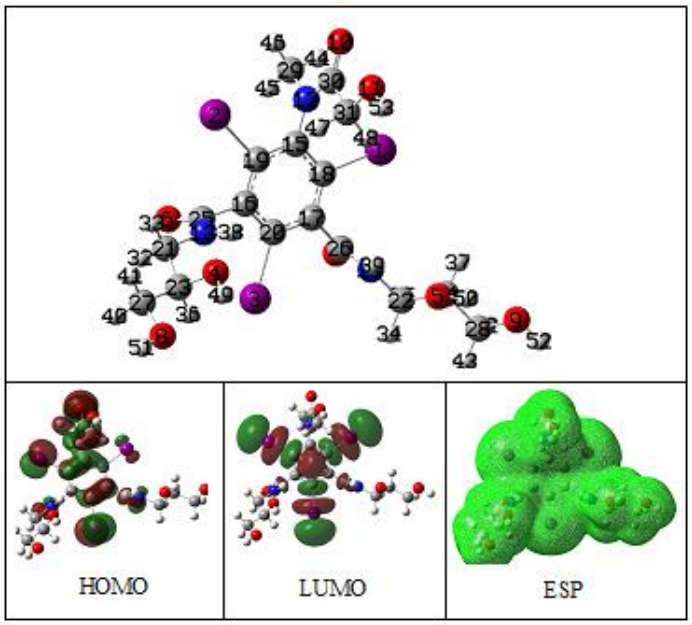

Figure 1. Optimized structure, HOMO, LUMO and total electron density map of Iomeprol

In Koopman's hypothesis, ionization potentials (IP) and electron affinities (EA) of the molecule are related with E_{HOMO} and E_{LUMO}. The electron affinity (EA) and ionization potential (IP) measure the tendency of compounds to gain or lose an electron [12]. The energy of frontier orbitals are presented in Figure 2. The higher the E_{HOMO}, the easier it is to remove an electron to form an ion.

In the Figure 2, the solvents are arranged in ascending order of dielectric constant with their respective values for E_{HOMO} and E_{LUMO} and near five molecular orbital energies close to frontier orbitals in eV unit.

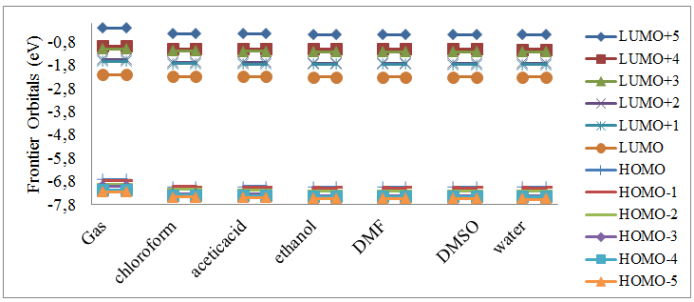

Figure 2. Frontier orbital energies for Iomeprol

We find that the inclusion of solvents causes the HOMO values become more negative and LUMO values become more positive due to the increase dielectric constant.

In Figure 2, it can be observed that it is more difficult to remove an electron from water > DMSO > DMF > ethanol > acetic acid > chloroform > gas phase to form an ion. Similarly, it is more difficult to add an electron in terms of their EAs to the molecule in gas phase > chloroform > acetic acid > ethanol > DMF > DMSO > water.

Compounds with large E_{HOMO}-E_{LUMO} gap value given with equation 3 tend to have higher stability [13].

$$E_{gap} = E_{LUMO} - E_{HOMO} \approx IP - EA \quad (3)$$

The kinetic stability, chemical reactivity, optical polarizability and chemical hardness-softness of a molecule are determined with the use of energy gap between E_{HOMO} and E_{LUMO}[14]. According to energy gap value, the order of stability of the molecule is more in the water > DMSO > DMF > ethanol > acetic acid > chloroform > gas phase. Interestingly, the order of stability for Iomeprol molecule increases with an increase in polarity of the solvents.

E_{HOMO}, E_{LUMO}, hardness, softness, electronegativity, chemical potential, electrophilicity index, nucleofugality, electrofugality, maximum electrons transferred in a chemical reaction in Iomeprol are shown in Table 1.

Chemical hardness is given by half of the energy band gap as shown in the equation 4 [15].

$$\eta = \frac{IP-EA}{2} \quad (4)$$

As seen in Table 1, Iomeprol molecule in the water phase has slightly the highest value of chemical hardness (2.381) is considered to be harder and more stable than in the rest of the solvents, followed by DMSO, DMF, ethanol, acetic acid and chloroform. This indicates that Iomeperol in chloroform is less stable than in the rest of the solvents.

Table 1. Chemical Parameters for Iomeperol

Solvent (ε)	E_{HOMO}	E_{LUMO}	ΔE	η	S	χ	μ	ω	ΔN_{max}	ΔE_n	ΔE_e
Gas	-6.746	-2.199	4.548	2.274	0.220	4.472	-4.472	4.399	1.967	1.063	10.008
Chloroform (4.81)	-7.018	-2.287	4.731	2.366	0.211	4.652	-4.652	4.574	1.967	1.105	10.409
Acetic acid (6.15)	-7.034	-2.294	4.740	2.370	0.211	4.664	-4.664	4.589	1.968	1.110	10.437
Ethanol (24.55)	-7.069	-2.310	4.759	2.379	0.210	4.689	-4.689	4.621	1.971	1.121	10.500
DMF (36.71)	-7.073	-2.312	4.761	2.380	0.210	4.692	-4.692	4.625	1.971	1.123	10.507
DMSO (46.68)	-7.074	-2.313	4.761	2.381	0.210	4.693	-4.693	4.626	1.971	1.123	10.510
Water (80.1)	-7.07 7	-2.314	4.763	2.381	0.210	4.695	-4.695	4.629	1.972	1.124	10.515

ε : Dielectric constant, ΔE: Energy gap, η: Hardness, S: Softness, χ: Electronegativity, μ: Chemical potential, ω: Electrophilicity index, ΔN_{max}: The maximum number of electrons transferred in a chemical reaction , ΔE_n: Nucleofugality, ΔEe:Electrofugality

As seen in Table 1, Iomeprol molecule in the water phase has slightly the highest value of chemical hardness (2.381) is considered to be harder and more stable than in the rest of the solvents, followed by DMSO, DMF, ethanol, acetic acid and chloroform with chemical hardness. This indicates that Iomeprol in chloroform is less stable than in the rest of the solvents.

Electron polarizability (i.e. chemical softness (S) refers to the capacity of an atom or an atom group to have electrons can be formulated with the equation 5.

$$S = \frac{1}{2\eta} = \left(\frac{\partial^2 N}{\partial E^2}\right)_{V(r)} = \left(\frac{\partial N}{\partial \mu}\right)_{V(r)} \quad (5)$$

Electrophilicity index (ω) refers to the measurement of energy decrease because of maximal electron flow between donor and acceptor. Global electrophilicity index (ω) is predicted by employing electronegativity and chemical hardness parameters in the equation [16, 13].

$$\omega = \frac{\mu^2}{2\eta} \quad (6)$$

High electrophilicity shows a good electrophile, and small electrophilicity shows a good nucleophile. As seen in Table 1, electrophilicity index increases with an increase in the dielectric constant of the solvents.

Electric dipole polarizability (measurement of linear response of an infinitesimal electric field (F) representing second-order variation energy is an important property used in determining the polarizability of a molecule or compound [17].

Mean polarizability ($\langle\alpha\rangle$), anisotropic polarizability ($\Delta\alpha$) and κ anisotropy, which are large experimental interest quantities in the theory of optoelectronic and intermolecular forces, of the molecule in gas and in various solvents were computed and reported in Table 2.

Table 2. Polarizability ($\langle\alpha\rangle$), Anisotropic Polarizability ($\Delta\alpha$), κ Anisotropy of the Optimized Iomeprol Molecule in the Gas Phase and Different Solvents

Solvent (ε)	<α>	<Δα> Esu 10^{-24}	<Δα> (Ure times)	κ
Gas	300	18.619	8.718	0.018
Chloroform (4.81)	368	22.495	10.533	0.017
Acetic acid (6.15)	374	22.858	10.703	0.017
Ethanol (24.55)	388	23.765	11.127	0.016
DMF (36.71)	390	23.873	11.178	0.016
DMSO (46.68)	390	23.918	11.199	0.016
Water (80.1)	391	23.989	11.232	0.016

It can also be observed that ongoing from non-polar to polar solvent the polarizability of Iomeprol increases as the polarity of the solvents decreases whereas the anisotropic polarizability increases with an increase in the polarity of the solvents. Consequently, the polarity of the solvents plays an important role in determining the values of the non-linear optical properties of Iomeprol. Urea is commonly used as a reference material in NLO studies. The calculated Δα, value for urea with the B3LYP/6-311++G(d,p) level is $2.13568262.10^{-24}$ esu [18]. As seen Table 2, the anisotropy of polarizability values for the title compound are approximately ten times greater than those of urea for gas and all solvents.

Hyperpolarizability is of boundary molecular orbital energies that aid in the use of intramolecular charge transfer to account for hyperpolarizability. In this study, the values of the first hyperpolarizability were obtained using the following equations:

The first order hyperpolarizability (β) such as βvec (β vector), β‖ (β parallel) and βtot (β total) is the nonlinear optical activity measurement. It is a 3rd rank tensor and may be described with 3×3×3 matrix and using Kleinman's symmetry, the 3D matrix is reduced to 27 components and 10 components. 10 components of this matrix that is called as β_{xxx}, β_{xxy}, β_{xyy}, β_{yyy}, β_{xxz}, β_{xyz}, β_{yyz}, β_{xzz}, β_{yzz}, β_{zzz} are provided output of GAUSSIAN calculations [19-21].

As the experimental first hyperpolarizability of Iomeprol values in the literature are not reported, it is hard to determine which basis set computes reliable β values. As the polarizability values α and the 1st hyperpolarizability β of Gaussian 09 are reported as atomic units (a.u.), the computed values were converted into electrostatic units (esu) (α: 1a.u.= 0.1482×10^{-24} esu; β: 1a.u.= 8.6393×10^{-33} esu). β_{xxx}, β_{xxy}, β_{xyy}, β_{yyy}, β_{xxz}, β_{xyz}, β_{yyz}, β_{xzz}, β_{yzz}, β_{zzz} matrix element are given in Table 3 and the total including the hyperpolarizability (βtot) which may be computed with the equation given below:

Here,

$\beta_x = \beta_{xxx} + \beta_{xyy} + \beta_{xzz}$

$\beta_y = \beta_{yyy} + \beta_{xxy} + \beta_{yzz}$ $\qquad \beta_{tot} = (\beta_x^2 + \beta_y^2 + \beta_z^2)^{1/2}$ (7)

$\beta_z = \beta_{zzz} + \beta_{xxz} + \beta_{yyz}$

Table 3: $\beta\times10^{-30}$ (esu), β (a.u.) Components and Values Calculated Using DFT Levels of Theory for Iomeprol

	Gas	Chloroform	Acetic Acid	Ethanol	DMF	DMSO	Water
β_{xxx}	-53.80	-89.30	-92.67	-101.90	-103.07	-103.57	-104.33
β_{xxy}	-96.50	-128.77	-134.12	-149.15	-151.11	-151.94	-153.26
β_{xyy}	6.54	48.58	53.67	67.03	68.71	69.42	70.55
β_{yyy}	-95.94	-2.83	9.86	44.13	48.48	50.30	53.19
β_{xxz}	6.27	-65.98	-73.66	-93.24	-95.73	-96.78	-98.47
β_{xyz}	-16.07	-8.45	-7.37	-4.49	-4.14	-3.99	-3.73
β_{yyz}	-79.96	-121.50	-125.53	-135.42	-136.61	-137.11	-137.94
β_{xzz}	12.97	32.52	34.42	38.69	39.26	39.51	39.93
β_{yzz}	2.60	63.84	70.78	88.64	90.83	91.76	93.24
β_{zzz}	25.30	55.53	58.98	68.02	69.13	69.56	70.14
β_{total}	1.72	1.28	1.30	1.40	1.41	1.42	1.44
β_{total} (ure times)	**2.38**	**1.77**	**1.80**	**1.94**	**1.95**	**1.97**	**1.97**

In Table 3, it is seen that the calculated β values of Iomeprol using B3lyp/lanl2dz level (the β of Iomeprol for gas, chloroform, acetic acid, ethanol, DMF, DMSO, water) are $1.72x10^{-30}$ esu., $1.28x10^{-30}$ esu., $1.30x10^{-30}$ esu., $1.40x10^{-30}$ esu., $1.41x10^{-30}$ esu., $1.42x10^{-30}$ esu., $1.44x10^{-30}$ esu. respectively. The first polarizability values obtained using B3lyp/lanl2dz level for Iomeprol are the largest value in gas phase and the lowest value in chloroform. Similarly β_{total} -first hyperpolarizability value is very important key factors to identify NLO properties of molecular systems. In all phase, the first hyperpolarizability values for the title compound are approximately two times greater than those of urea (β_{total}, value for urea with the B3LYP/6-311++G(d,p) level is $7.2228469891.10^{-31}$ esu [18]). Due to the obtained results, the Iomeprol molecule has bigger first hyperpolarizability than urea. So, it may be an attractive matter for the nonlinear optical applicants.

NBO analysis emphasizing the intermolecular orbital interaction's role in charge transfer is done by considering all probable interactions among the donor and receiver NBOs and by predicting energetic significance with second-order perturbation theory. For donor NBO (i) and acceptor NBO (j), the stabilization energy E(2) attributed to electron delocalization between the donor and the receiver is predicted below:

$$E^{(2)} = q_i \frac{(F_{i,j})^2}{\varepsilon_j - \varepsilon_i} \quad (8)$$

where $F_{i,j}$ is the o-diagonal NBO Fock matrix element, q_i is the orbital occupancy, and ε_i, ε_j are diagonal elements conjugative interactions in molecular system [22].

Delocalization of electron density between occupied Lewis type (bond or lone pair) NBO orbitals and formally unoccupied (antibonding or Rydberg) non Lewis NBO orbital's correspond to a stabling donor-acceptor inter-action. The molecular interaction is formed by the orbital overlap between.

When $E^{(2)}$ value becomes large, it shows that the interaction between electron donors and acceptors is intensive, and when the donation tendency from electron donors to electron acceptors is more, the extent of conjugation of the whole system is larger [23].

Table 4: Second-order perturbation theory analysis of Fock matrix in NBO basis for Iomeprol are listed in Table 4 and 5, and 6 which incukdes only energy fort he other studied solvent.

The energies for the interaction n3(I_1) → π*(C_{15}-C_{18}) , n3(I_2) → π*(C_{16}-C_{19}) and n3(I_3) → (C_{17}-C_{20}) 7.72, 7.83 and 7.49 $kcalmol^{-1}$, respectively demonstrate the intramolecular hyperconjugative interaction between the iodine atoms and benzene ring is strong in the ground state for Iomeprol in gas phase. The energies for the interaction n3(I_1) → π*(C_{15}-C_{18}), n3(I_2) → π*(C_{16}-C_{19}) and n3(I_3) → (C_{17}-C_{20}) becomes 7.81, 7.59 and $kcalmol^{-1}$, respectively in water phase (Table 5). The energies for the interaction are 20.81 and 19.22 $kcalmol^{-1}$ for n2(O_6) → σ*(N_{13}-C_{25}), and σ*(C_{16}-C_{25}); 20.87 and 19.18 $kcalmol^{-1}$ for n2(O_7) → σ*(N_{14}-C_{26}) and (C_{17}-C_{26}); 24.14 $kcalmol^{-1}$ for n2(O_7) → σ*(N_{12}-C_{30}). The highest energies for the interaction are seen as 57.29 $kcalmol^{-1}$ for n1(N_{12}) → σ*(O_{10}-C_{30}) in gas phase.

Table 4. Second-order Perturbation Theory Analysis of Fock Matrix in NBO Basis for Iomeprol for Gas Phase

Donor(i)	Type	Occupancy	ED(j)	Acceptor	Type	Occupancy	ED(j)	E(2) kcal/mol	E(j)-E(i) a.u	F(i,j) a.u
I_1-C_{18}	σ	1.965	-0.515	C_{15}-C_{19}	σ*	0.049	0.481	7.45	1	0.077
I_1-C_{18}	σ	1.965	-0.515	C_{17}-C_{20}	σ*	0.039	0.489	7.16	1	0.076
I_2-C_{19}	σ	1.965	-0.514	C_{15}-C_{18}	σ*	0.049	0.482	7.5	1	0.077
I_2-C_{19}	σ	1.965	-0.514	C_{16}-C_{20}	σ*	0.039	0.490	7.19	1	0.076
I_3-C_{20}	σ	1.967	-0.518	C_{16}-C_{19}	σ*	0.039	0.495	7.12	1.01	0.076
I_3-C_{20}	σ	1.967	-0.518	C_{17}-C_{18}	σ*	0.039	0.495	7.15	1.01	0.076
C_{15}-C_{18}	π	1.668	-0.301	C_{16}-C_{19}	π*	0.388	-0.009	18.87	0.29	0.067
C_{15}-C_{18}	π	1.668	-0.301	C_{17}-C_{20}	π*	0.393	-0.010	23	0.29	0.074
C_{16}-C_{19}	π	1.665	-0.298	C_{15}-C_{18}	π*	0.402	-0.017	22.73	0.28	0.073
C_{16}-C_{19}	π	1.665	-0.298	C_{17}-C_{20}	π*	0.393	-0.010	19.03	0.29	0.067
C_{16}-C_{25}	σ	1.959	-0.662	N_{13}-C_{21}	σ*	0.022	0.307	5.85	0.97	0.068
C_{17}-C_{18}	σ	1.962	-0.747	N_{12}-C_{15}	σ*	0.043	0.356	4.92	1.1	0.066
C_{17}-C_{20}	π	1.669	-0.298	C_{15}-C_{18}	π*	0.402	-0.017	19.64	0.28	0.068
C_{17}-C_{20}	π	1.669	-0.298	C_{16}-C_{19}	π*	0.388	-0.009	23.5	0.29	0.075
C_{17}-C_{26}	σ	1.959	-0.663	N_{14}-C_{22}	σ*	0.023	0.304	5.87	0.97	0.068
C_{30}-C_{31}	σ	1.977	-0.632	N_{12}-C_{29}	σ*	0.025	0.286	5.49	0.92	0.063
C_{31}-H_{48}	σ	1.974	-0.524	O_{10}-C_{30}	π*	0.260	0.003	4.98	0.53	0.049
I_1	n3	1.933	-0.273	C_{15}-C_{18}	π*	0.402	-0.017	7.72	0.26	0.044
I_2	n3	1.931	-0.273	C_{16}-C_{19}	π*	0.388	-0.009	7.83	0.26	0.044
I_3	n3	1.940	-0.277	C_{17}-C_{20}	π*	0.393	-0.010	7.49	0.27	0.044
O4	n2	1.965	-0.336	C_{23}-C_{27}	σ*	0.031	0.332	5.69	0.67	0.055
O_5	n2	1.966	-0.337	C_{24}-C_{28}	σ*	0.031	0.331	5.67	0.67	0.055

O_6	n2	1.866	-0.257	N_{13}-C_{25}	σ*	0.072	0.426	20.81	0.68	0.108
O_6	n2	1.866	-0.257	C_{16}-C_{25}	σ*	0.074	0.359	19.22	0.62	0.099
O_7	n2	1.867	-0.259	N_{14}-C_{26}	σ*	0.072	0.424	20.87	0.68	0.108
O_7	n2	1.867	-0.259	C_{17}-C_{26}	σ*	0.074	0.358	19.18	0.62	0.099
O_8	n2	1.972	-0.348	C_{27}-H_{40}	σ*	0.021	0.429	5.71	0.78	0.06
O_9	n2	1.972	-0.347	C_{28}-H_{42}	σ*	0.021	0.429	5.66	0.78	0.059
O_{10}	n2	1.863	-0.233	N_{12}-C_{30}	σ*	0.088	0.401	24.14	0.63	0.112
O_{10}	n2	1.863	-0.233	C_{30}-C31	σ*	0.074	0.344	20.3	0.58	0.098
O_{11}	n2	1.967	-0.283	C_{31}-H_{47}	σ*	0.025	0.440	5.84	0.72	0.058
O_{11}	n2	1.967	-0.283	C_{31}-H_{48}	σ*	0.025	0.439	5.64	0.72	0.057
N_{12}	n1	1.721	-0.260	O_{10}-C_{30}	π*	0.260	0.003	57.29	0.26	0.11
N_{12}	n1	1.721	-0.260	C_{15}-C_{18}	σ*	0.049	0.482	7.51	0.74	0.071
N_{12}	n1	1.721	-0.260	C_{15}-C_{19}	σ*	0.049	0.481	7.31	0.74	0.07
N_{13}	n1	1.668	-0.267	O_6-C_{25}	σ*	0.265	0.083	40.51	0.35	0.108
N_{13}	n1	1.668	-0.267	O_6-C_{25}	π*	0.085	0.373	5.31	0.64	0.056
N_{13}	n1	1.668	-0.267	C_{21}-H_{33}	σ*	0.024	0.448	6.24	0.72	0.065
N_{14}	n1	1.669	-0.269	O_7 -C_{26}	σ*	0.244	0.113	33.44	0.38	0.103
N_{14}	n1	1.669	-0.269	O_7 -C_{26}	π*	0.105	0.340	7.42	0.61	0.064
N_{14}	n1	1.669	-0.269	C_{22}-H_{34}	σ*	0.024	0.442	6.31	0.71	0.065

Table 5. Second-order Perturbation Theory Analysis of Fock Matrix in NBO Basis for Iomeprol for Water Phase

Item NO	**Iomeprol-water**									
	Donor (i)	**Type**	**Occup.**	**ED(j)**	**Acceptor**	**Type**	**Occup.**	**ED(j)**	**E(2) kcal/mol**	**E(j)-E(i) a.u**	**F(i,j) a.u**
1	I_1-C_{18}	σ	1.965	-0.519	C_{15}-C_{19}	σ*	0.048	0.478	7.49	1	0.077
1	I_1-C_{18}	σ	1.965	-0.519	C_{17}-C_{20}	σ*	0.039	0.483	7.24	1	0.076
2	I_2-C_{19}	σ	1.964	-0.518	C_{15}-C_{18}	σ*	0.048	0.478	7.54	1	0.078
2	I_2-C_{19}	σ	1.964	-0.518	C_{16}-C_{20}	σ*	0.039	0.484	7.26	1	0.076
3	I_3-C_{20}	σ	1.967	-0.524	C_{16}-C_{19}	σ*	0.039	0.490	7.14	1.01	0.076
3	I_3-C_{20}	σ	1.967	-0.524	C_{17}-C_{18}	σ*	0.039	0.490	7.17	1.01	0.076
28	N14-H39	σ	1.983	-0.672	O 7-C26	π*	0.030	0.436	5.1	1.11	0.067
30	C_{15}-C_{18}	π	1.668	-0.306	C_{16}-C_{19}	π*	0.387	-0.014	19.27	0.29	0.068
30	C_{15}-C_{18}	π	1.668	-0.306	C_{17}-C_{20}	π*	0.393	-0.016	22.87	0.29	0.074
33	C_{16}-C_{19}	π	1.662	-0.302	C_{15}-C_{18}	π*	0.400	-0.022	22.61	0.28	0.072
33	C_{16}-C_{19}	π	1.662	-0.302	C_{17}-C_{20}	π*	0.393	-0.016	19.51	0.29	0.068
38	C_{17}-C_{20}	π	1.670	-0.304	C_{15}-C_{18}	π*	0.400	-0.022	19.83	0.28	0.068
38	C_{17}-C_{20}	π	1.670	-0.304	C_{16}-C_{19}	π*	0.387	-0.014	23.19	0.29	0.074
39	C_{17}-C_{26}	σ	1.959	-0.672	N_{14}-C_{22}	σ*	0.023	0.297	6.04	0.97	0.069
50	C_{27}-H_{40}	σ	1.983	-0.526	O $_4$-C_{23}	σ*	0.032	0.211	5.01	0.74	0.054
52	C28-H42	σ	1.983	-0.528	O 5-C24	σ*	0.032	0.210	4.99	0.74	0.054
57	C_{30}-C_{31}	σ	1.977	-0.646	N_{12}-C_{29}	σ*	0.025	0.274	5.76	0.92	0.065
59	C_{31}-H_{48}	σ	1.972	-0.526	O_{10}-C_{30}	π*	0.294	-0.022	5.15	0.5	0.049
90	I_1	3	1.933	-0.279	C_{15}-C_{18}	π*	0.400	-0.022	7.81	0.26	0.044
93	I_2	3	1.931	-0.277	C_{16}-C_{19}	π*	0.387	-0.014	7.89	0.26	0.044
96	I_3	3	1.942	-0.287	C_{17}-C_{20}	π*	0.393	-0.016	7.39	0.27	0.044
98	O_4	2	1.967	-0.337	C_{23}-C_{27}	σ*	0.029	0.346	5.36	0.68	0.054
100	O_5	2	1.968	-0.342	C_{24}-C_{28}	σ*	0.029	0.344	5.37	0.69	0.054

102	O_6	2	1.880	-0.275	N_{13}-C_{25}	σ*	0.066	0.433	19.32	0.71	0.106
102	O_6	2	1.880	-0.275	C_{16}-C_{25}	σ*	0.071	0.351	17.91	0.63	0.096
104	O_7	2	1.881	-0.277	N_{14}-C_{26}	σ*	0.066	0.431	19.42	0.71	0.106
104	O_7	2	1.881	-0.277	C_{17}-C_{26}	σ*	0.071	0.350	17.94	0.63	0.096
106	O_8	2	1.971	-0.342	C_{27}-H_{40}	σ*	0.020	0.455	5.81	0.8	0.061
108	O_9	2	1.971	-0.342	C_{28}-H_{42}	σ*	0.020	0.455	5.81	0.8	0.061
110	O_{10}	2	1.880	-0.258	N_{12}-C_{30}	σ*	0.080	0.404	21.92	0.66	0.109
110	O_{10}	2	1.880	-0.258	C_{30}-C31	σ*	0.067	0.337	18.44	0.6	0.095
112	O_{11}	2	1.970	-0.296	C_{31}-H_{47}	σ*	0.023	0.448	5.41	0.74	0.057
112	O_{11}	2	1.970	-0.296	C_{31}-H_{48}	σ*	0.023	0.446	5.33	0.74	0.056
113	N_{12}	1	1.699	-0.273	O_{10}-C_{30}	σ*	0.294	-0.022	65.95	0.25	0.115
113	N_{12}	1	1.699	-0.273	C_{15}-C_{18}	σ*	0.048	0.478	7.06	0.75	0.07
113	N_{12}	1	1.699	-0.273	C_{15}-C_{19}	σ*	0.048	0.478	6.9	0.75	0.069
114	N_{13}	1	1.635	-0.272	O_6-C_{25}	σ*	0.369	-0.041	86.43	0.23	0.126
114	N_{13}	1	1.635	-0.272	C_{21}-H_{33}	σ*	0.022	0.457	6.05	0.73	0.065
115	N_{14}	1	1.637	-0.274	O_7 -C_{26}	σ*	0.358	-0.030	78.91	0.24	0.124
115	N_{14}	1	1.637	-0.274	C_{22}-H_{34}	σ*	0.023	0.450	6.22	0.72	0.066

Table 6. Interaction Energies of Iomeprol for Different Solvent

Donor (i)	Type	Acceptor	Type	Gas	Chloroform	Acetic Acid	Ethanol	DMF	DMSO	Water
				E(2) kcal/mol						
I_1-C_{18}	σ	C_{15}-C_{19}	σ*	7.45	7.48	7.48	7.49	7.49	7.49	7.49
I_1-C_{18}	σ	C_{17}-C_{20}	σ*	7.16	7.22	7.22	7.23	7.23	7.23	7.24
I_2-C_{19}	σ	C_{15}-C_{18}	σ*	7.5	7.53	7.53	7.54	7.54	7.54	7.54
I_2-C_{19}	σ	C_{16}-C_{20}	σ*	7.19	7.24	7.25	7.26	7.26	7.26	7.26
I_3-C_{20}	σ	C_{16}-C_{19}	σ*	7.12	7.13	7.13	7.14	7.14	7.14	7.14
I_3-C_{20}	σ	C_{17}-C_{18}	σ*	7.15	7.17	7.17	7.17	7.17	7.17	7.17
N_{13}-H_3	σ	O_6-C_{25}	π*		5.12	5.16	5.24	5.25	5.25	
N_{14}-H_{39}	σ	O_7-C_{26}	π*					5.08	5.09	5.1
C_{15}-C_{18}	π	C_{16}-C_{19}	π*	18.87	19.18	19.20	19.26	19.27	19.27	19.27
C_{15}-C_{18}	π	C_{17}-C_{20}	π*	23	22.90	22.90	22.87	22.87	22.87	22.87
C_{16}-C_{19}	π	C_{15}-C_{18}	π*	22.73	22.64	22.63	22.61	22.61	22.61	22.61
C_{16}-C_{19}	π	C_{17}-C_{20}	π*	19.03	19.40	19.42	19.49	19.50	19.50	19.51
C_{16}-C_{25}	σ	N_{13}-C_{21}	σ*	5.85	5.96	5.97		5.99	5.99	
C_{17}-C_{18}	σ	N_{12}-C_{15}	σ*	4.92	5.00	5.00		19.83	5.02	
C_{17}-C_{20}	π	C_{15}-C_{18}	π*	19.64	19.79	19.80	19.83	23.19	19.83	19.83
C_{17}-C_{20}	π	C_{16}-C_{19}	π*	23.5	23.26	23.24	23.20	6.03	23.19	23.19
C_{17}-C_{26}	σ	N_{14}-C_{22}	σ*	5.87	6.00	6.01	6.03	5.01		6.04
C_{27}-H_{40}	σ	O $_4$-C_{23}	σ*				5.00		5.01	5.01
C_{30}-C_{31}	σ	N_{12}-C_{29}	σ*	5.49	5.69			5.75		5.76
C_{31}-H_{48}	σ	O_{10}-C_{30}	π*	4.98		5.09	5.14			5.15
I_1	3	C_{15}-C_{18}	π*	7.72	7.79	7.80	7.81	7.81	7.81	7.81
I_2	3	C_{16}-C_{19}	π*	7.83	7.87	7.87	7.88	7.88	7.88	7.89
I_3	3	C_{17}-C_{20}	π*	7.49	7.41	7.41	7.39	7.39	7.39	7.39
O_4	2	C_{23}-C_{27}	σ*	5.69		5.43	5.37	5.37	5.38	5.36
O_5	2	C_{24}-C_{28}	σ*	5.67	5.46		5.39	5.38		5.37
O_6	2	N_{13}-C_{25}	σ*	20.81	19.68	19.59	19.37	19.35	19.34	19.32
O_6	2	C_{16}-C_{25}	σ*	19.22	18.24	18.16	17.96	17.93	17.93	17.91
O_7	2	N_{14}-C_{26}	σ*	20.87	19.77	19.68	19.47	19.44	19.43	19.42
O_7	2	C_{17}-C_{26}	σ*	19.18	18.26	18.18	17.99	17.97	17.96	17.94
O_8	2	C_{27}-H_{40}	σ*	5.71	5.80	5.81	5.81	5.81	5.81	5.81
O_9	2	C_{28}-H_{42}	σ*	5.66	5.79	5.80		5.81	5.81	5.81
O_{10}	2	N_{12}-C_{30}	σ*	24.14	22.43	22.30	21.99	21.96		21.92

O_{10}	2	C_{30}-C31	σ*	20.3	18.89	18.78	18.50	18.47		18.44
O_{11}	2	C_{31}-H_{47}	σ*	5.84	5.51	5.48		5.42	5.42	5.41
O_{11}	2	C_{31}-H_{48}	σ*	5.64	5.42	5.40		5.34	5.34	5.33
N_{12}	1	O_{10}-C_{30}	π*	57.29	63.81	64.36	65.65	65.79	65.86	65.95
N_{12}	1	C_{15}-C_{18}	σ*	7.51	7.16	7.13	7.07	7.06	7.06	7.06
N_{12}	1	C_{15}-C_{19}	σ*	7.31	7.01	6.98	6.92	6.91	6.91	6.9
N_{13}	1	O_6-C_{25}	σ*	40.51	82.56	83.67	85.92	86.17	86.27	86.43
N_{13}	1	O_6-C_{25}	π*	5.31						
N_{13}	1	C_{21}-H_{33}	σ*	6.24	6.12	6.10	6.06	6.06	6.05	6.05
N_{14}	1	O_7 -C_{26}	σ*	33.44	70.19	72.49	77.75	78.33	78.56	78.91
N_{14}	1	O_7 -C_{26}	π*	7.42						
N_{14}	1	C_{22}-H_{34}	σ*	6.31	6.27	6.26	6.23	6.22	6.22	6.22

Table 6 shows that the variation of the first hyperpolarizability of Iomeprol for different solvents. Seen as for n1(N_{12}) → σ*(O_{10}-C_{30}) interaction in gas phase being 57.29 kcalmol^{-1} increases with the polarity of the solvents increases. The order of this interaction is more in chloroform > acetic acid > ethanol > DMF > DMSO > water (Table 6). The same order are observed for n1(N_{13}) → σ*(O_6-C_{25}) interaction. These interaction are 40.51, 82.56, 83.67, 85.92, 86.17 and 86.27 kcalmol^{-1} in gas, chloroform, acetic acid, ethanol, DMF, DMSO and water. n1(N14) → σ*(O7 -C26) interaction energies are 33.44, 70.19, 72.49, 77.75, 78.33, 78.56 kcalmol^{-1}.

4. Conclusions and Recommendations

The molecular structures and quantum chemical parameters of the Iomeprol in different solvents were studied by employing the B3LYP with the lanl2dz basis set. To understand the effects of solvents on structural, electronic and non-linear optical properties of Iomeprol molecule, extensive computational study of the HOMO, LUMU, HOMO-LUMO energy gap, ionization potential, electron affinity, chemical hardness, chemical softness, chemical potential, electronegativity, electrophilicity index polarizability, anisotropic polarizability, hyperpolarizability were calculated. Quantum chemical parameters for Iomeprol in different solvents were investigated by determining the polarizability α and the hyperpolarizability β by employing the same methods.

It was determined in the study that the energy gap hardness increases with the incese of dielectric contant of the solvent interaction energy. The polarizability and the anisotropic polarizability increases with the increase in the dielectric constant of the solvents while κ anisotropy decreases as the polarity of the solvents increases. The title molecule may be an attractive in the future nonlinear optical materials studies according to anisotropic polarizability and hyperpolarizability values. In the NBO analysis, it was observed interaction between donor and acceptor electrons change with the change of dielectric constant of the solvent.

References

[1] Singh, J., & Daftary, A. (2008). Iodinated contrast media and their adverse reactions. Journal of nuclear medicine technology, 36(2), 69-74.

[2] Almen, T. (1994). The etiology of contrast medium reactions. Investigative radiology, 29, S37-S45.

[3] Dooley, M., & Jarvis, B. (2000). Iomeprol. Drugs, 59(5), 1169-1186.

[4] Lorusso V, Taroni P, Alvino S, Sipinazzi A. (2001). Pharmacokinetics and safety of iomeprol in healthy volunteers and in patients with renal impairment or end-stage renal disease requiring hemodialysis. Investigative radiology, 36(6), 309-316.

[5] Rosati, G. (1994). Clinical pharmacology of iomeprol. European journal of radiology, 18, S51-S60.

[6] Fattori, R., Piva, R., Schicchi, F., Pancrazi, A., Gabrielli, G., Marzocchi, A., ... & Magnani, B. (1994). Iomeprol and iopamidol in cardiac angiography: a randomised, double-blind, parallel-group comparison. European journal of radiology, 18, S61-S66.

[7] Rosati, G. (1994). Clinical utility and safety profile of iomeprol. European journal of radiology, 18, S120-S124.

[8] Frisch, M.J., Trucks, G.W., Schlegel, H.B., Scuseria, G.E., Robb, M.A., Cheeseman, J.R., Scalmani, G., Barone, V., Mennucci, B., Petersson, G.A., Nakatsuji, H., Caricato, M., Li, X., Hratchian, H.P., Izmaylov, A.F., Bloino, J., Zheng, G., Sonnenberg, J.L., Hada, M., Ehara, M., Toyota, K., Fukuda, R., Hasegawa, J., Ishida, M., Nakajima, T., Honda, Y., Kitao, O., Nakai, H., Vreven, T., Montgomery, J.A. Jr., Peralta, J.E., Ogliaro, F., Bearpark, M., Heyd, J.J., Brothers, E., Kudin, K.N., Staroverov, V.N., Keith, T., Kobayashi, R., Normand, J., Raghavachari, K., Rendell, A., Burant, J.C., Iyengar, S.S., Tomasi, J., Cossi, M., Rega, N., Millam, J.M., Klene, M., Knox, J.E., Cross, J.B., Bakken, V., Adamo, C., Jaramillo, J., Gomperts, R., Stratmann, R.E., Yazyev, O., Austin, A.J., Cammi, R., Pomelli, C., Ochterski, J.W., Martin, R.L., Morokuma, K., Zakrzewski, V.G., Voth, G.A., Salvador, P., Dannenberg, J.J., Dapprich, S., Daniels, A.D., Farkas, O., Foresman, J.B., Ortiz, J.V., Cioslowski, J., Fox, D.J.: Gaussian09 Revision D. 01, Gaussian Inc. Wallingford CT (2009)

[9] Dennington, R., Keith, T., Millam, J.: GaussView, version 5 (2009).

[10] Becke, A. D. (1992). Density-functional thermochemistry. I. The effect of the exchange-only gradient correction. The Journal of chemical physics, 96(3), 2155-2160.

[11] Mekky, A. H., Elhaes, H. G., El-Okr M. M., Al-Aboodi, A. S., Ibrahim, M.A. (2015). Effect of Solvents on the Electronic Properties of Fullerene Based Systems : Molecular Modelling. Journal of Applied Computational. Mathematics 4(1),1–4.

[12] Kumer, A., Ahmed, B., Sharif, M. A., & Al-Mamun, A. (2017). A theoretical study of aniline and nitrobenzene by computational overview. Asian Journal of Physical and Chemical Sciences, 1-12.

[13] Srivastava, K. K., Srivastava, S., & Alam, M. T. (2014). Theoretical study of the effects of solvents on the ground state of TCNQ. Pelagia Res. Libr, 5(1), 288-295.

[14] Pegu, D. (2014). Solvent effects on nonlinear optical properties of novel para-nitroaniline derivatives: A density functional approach. Int. J. Sci. Res, 3(7), 469-474.

[15] Oyeneyin, O. E. (2017). Structural and Solvent Dependence of the Electronic Properties and Corrosion Inhibitive Potentials of 1,3,4-thiadiazole and Its Substituted Derivatives-A Theoretical Investigation. Phys. Sci. Int. J. 16(2),1-8.

[16] Khan, M. F., Rashid, R. B., Hossain, M. A., & Rashid, M. A. (2017). Computational study of solvation free energy, dipole moment, polarizability, hyperpolarizability and molecular properties of Betulin, a constituent of Corypha taliera (Roxb.). Dhaka University Journal of Pharmaceutical Sciences, 16(1), 1-9.

[17] Abdulaziz, H., Gidado, A. S., Musa, A., & Lawal, A. (2019). Electronic Structure and Non-Linear Optical Properties of Neutral and Ionic Pyrene and Its Derivatives Based on Density Functional Theory. Journal of Materials Science Research and Reviews, 1-13.

[18] Sert, Y., Gümüş, M., Gökce, H., Kani, İ., Koca, İ. (2018).Molecular docking, Hirshfeld surface, structural, spectroscopic, electronic, NLO and thermodynamic analyses on novel hybrid compounds containing pyrazole and coumarin cores. Journal of Molecular Structure, 1171, 850-866.

[19] Prasad, P. N. (1991). Williams; DJ Introduction to Nonlinear Optical Effects in Organic Materials and Polymers.

[20] Machado, A. E., Neto, N. M., Ueno, L. T., de Paula, L. F., Araújo, D. M., Oliveira, G. S., ... & Oliveira-Campos, A. M. (2008). Study of the spectroscopic properties and first hyperpolarizabilities of disperse azo dyes derived from 2-amino-5-nitrothiazole. Journal of Photochemistry and Photobiology A: Chemistry, 199(1), 23-33.

[21] Kanis, D. R., Ratner, M. A., & Marks, T. J. (1994). Design and construction of molecular assemblies with large second-order optical nonlinearities. Quantum chemical aspects. Chemical Reviews, 94(1), 195-242.

[22] Snehalatha, M., Ravikumar, C., Joe, I. H., Sekar, N., & Jayakumar, V. S. (2009). Spectroscopic analysis and DFT calculations of a food additive Carmoisine. Spectrochimica Acta Part A: Molecular and Biomolecular Spectroscopy, 72(3), 654-662.

[23] Rui-Zhou, Z., Xiao-Hong, L., Xian-Zhou, Z. (2011). Molecular Structure, Vibrational Spectra and NBO Analysis on 1N-acetyl-3-(2, 4dichloro-5-fluoro-phenyl)-5-(p-methyl-phenyl)-2-pyrazoline Using DFT Method. Indian Journal of Pure&Applied Physics. 49(11),731-9.